Bulletin of the Seismological Society of America, 92, 1, pp. 339–349, February 2002

Space-Time Correlations of Seismotectonic Parameters: Examples from Japan and from Turkey Preceding the İzmit Earthquake

by Ali Osman Oncel and Thomas H. Wilson

Abstract Analysis of the correlation between fractal attributes of complex seismotectonic variables may offer insights into seismic hazard assessment. The Gutenberg–Richter, moment–magnitude, and moment–source area relations yield a direct fractal relationship among the Gutenberg–Richter *b*-value, occurrence rate, and the characteristic linear dimension of the fault plane (square root of fault surface area). In contrast, temporal variation in the correlation dimension of epicenters (D_C) is found, in several studies, to correlate negatively with the *b*-value in different regions of the world. Spatial variations between the *b*-value and D_C also tend to oppose each other. In Japan, negative correlations are also observed in the regional scale comparisons of the capacity dimension (D_o) of active fault systems and the *b*-value. However, at local scales, the relationship yields both positive and negative correlation. The occurrence of positive or negative correlation appears to be controlled by different modes of failure within the active fault complex.

Spatial variations between the *b*-value and D_C along the Northern Anatolian Fault Zone (NAFZ) suggest that, on average from 1900 to 1992, earthquake magnitudes were higher and epicenters more scattered within the central NAFZ than in its eastern and western segments. Temporal analysis reveals that the relationship between the *b*-value and D_C are nonstationary. Temporal correlations are generally negative. A period of positive correlation is observed between 1976 and 1988. During the last 3 yr of this period (1985–1988), both the *b*-value and D_C rose significantly, suggesting that stress release occurs through increased levels of low-magnitude and increasingly scattered seismicity. This dispersed pattern of seismicity, in combination with higher slip rates in the central NAFZ, may be one that did not adequately relieve stress along the main fault zone. This change in behavior and the tendency during the last century for the seismicity to migrate westward along the NAFZ may point to an increased risk of larger magnitude events such as the İzmit earthquake.

Introduction

Natural phenomena are often characterized by complex patterns that have similar appearance over several ranges of scale (Burrough, 1981; Korvin, 1992; Robertson and Sammis, 1995; Jiang and Plotnick, 1998). Examples include patterns formed by leaf veins, solute diffusion, and cloud shapes. Fractals have provided a way to characterize complex phenomena in a variety of disciplines ranging from the medical sciences to photogrammetry. Numerous examples of fractal characterization are encountered in the earth sciences. Analysis of topography, for example, suggests that it is fractal (e.g., Gilbert, 1989; Mareschal, 1989; Klinkberg and Goodchild, 1992). Tectonic processes are generally assumed to have fractal properties in both time and space (Aki, 1981; Rundle, 1989; Turcotte, 1989a,b; Wu, 1993; Cowie *et al.,* 1995; Godano and Caruso, 1995; Oncel, 1995, 1996a,b; Wilson and Dominic, 1998; Wilson, 2001). Surface fracture traces (Barton and Hsieh, 1989; Walsh and Watterson, 1993; Barton, 1994; Weiss and Gay, 1998) and active faults (Hirata, 1989a; Oncel *et al.,* 1995; Oncel and Alptekin, 1996; Oncel *et al.,* 2001; Wilson, 2001) form fractal patterns, and fractal models of fault systems predict the relative velocities along the main and higher-order fault strands (Turcotte, 1986).

Fault–Magnitude Interrelationships

Studies of possible correlation between earthquake seismicity and fault distribution are limited. The potential application to hazard assessment of fractal associations between seismotectonic variables lies mainly in the potential to distinguish between normal and anomalous correlations between the fractal attributes of these data sets. For example, Oncel *et al.* (2001) noted that a negative correlation between the b-value and D (active faults) observed in one area of Japan is associated with relatively low maximum magnitude earthquake activity. Yet, this area has lower b-values than elsewhere in Japan and coincides with an area of increased active fault complexity. The lower maximum magnitudes of earthquakes in this area may represent anomalous conditions. The coincidence of low maximum magnitude and low b-value may in itself suggest that historical earthquake activity in this area may not be representative of the potential for greater earthquakes. However, an active fault network of increasing complexity is present through the area along which larger magnitude earthquakes could occur. Mapping and analysis of these correlation patterns may provide insight into the earthquake mechanism and risk.

The relationship between the spatial distribution of faults and seismicity is anticipated from the interrelationships among the frequency–magnitude (Gutenberg and Richter, 1952), moment–magnitude (Aki, 1967), and moment–source area (Kanamori and Anderson, 1975). The result,

$$N = \beta r^{-2b}, \tag{1}$$

(see Turcotte, 1992) defines a fractal interrelationship among the frequency of earthquake occurrence (N), the characteristic linear dimension of the fault surface (r), and the b-value from the Gutenberg–Richter relationship ($\log N = -bm + a$), where β is a constant. Equation (1) defines a fractal relationship between N and r in which the fractal dimension, D, equals $2b$.

The spatial distribution of faults in central Japan has been shown by Hirata (1989a) to be fractal and to obey the following power law,

$$N = Cr^{-D}, \tag{2}$$

where N is the number of areas of size r that are occupied by parts of the fault pattern, and C is a constant of proportionality. Equation (2) suggests that cumulative fault length has a fractal distribution. In general, we would expect N of equation (1) to vary directly with N of equation (2), that is, the density of earthquakes in the subsurface is expected to vary in proportion to the density of active fault networks exposed at the surface.

Spatial–Magnitude Interrelationships

Hirata (1989a), Henderson *et al.* (1992), and Oncel (1995, 1996a,b) compared the fractal dimension of epicenter distribution with the b-value in the Gutenberg–Richter relation and obtained a negative correlation. This is the opposite of Aki's (1981) prediction that $D = 3b/c$. Hirata's (1989a) result reveals greater complexity in the relationship between earthquake distribution and b; however, several lines of reasoning suggest that Aki's prediction should hold (e.g., King, 1983; Turcotte, 1986). Further evaluation of the relationship proposed by Aki (1981) suggests that both positive and negative correlations exist between the fractal dimensions of active fault complexes and the b-value (Oncel *et al.,* 2000). A wide variety of phenomena exhibit scale-invariant spatial and temporal distribution, including fault and earthquake distribution and temporal patterns of earthquake occurrence. These observations suggest that many natural fracture systems and earthquake populations may be described and interpreted in terms of their fractal geometry (Mandelbrot, 1982). Other examples include fractal characterization of fracture patterns (Barton and Hseigh, 1985), fragmentation of the lithosphere (Turcotte, 1986), and the roughness of individual fault traces, such as the San Andreas in California (Aviles *et al.,* 1987; Okubo and Aki, 1987). Considerable work suggests that the fractal properties are scale limited (Scholz, 1995; Oncel *et al.,* 2001; Wilson, 2001).

Spatial patterns of earthquake distribution and temporal patterns of epicenter distribution are also demonstrated to be fractal by using the two-point correlation dimension D_C (e.g., Kagan and Knopoff, 1980; Sadovsky *et al.,* 1984). Similar observations have also been made of the fractal correlation dimension of laboratory scale seismicity associated with microfracturing in rocks (Mogi, 1962; Scholz, 1968; Hirata *et al.,* 1987; Main *et al.,* 1990). The Gutenberg–Richter b-value noted previously has been suggested to represent a generalized fractal dimension of earthquake magnitude distributions (Aki, 1981; Turcotte, 1992). Sornette *et al.* (1991) noted that this interpretation assumes a dislocation model for the seismic source and also requires a scale-invariant recurrence interval. The relationship has nevertheless been proven to apply on empirical grounds for tensile fracture in the laboratory (Hatton *et al.,* 1993). Whereas the significance of the relationship at a larger scale remains uncertain, the relationship is implicitly assumed in much of the recent literature on the nonlinear dynamics of earthquakes (Main, 1996). However, the b-value has been shown to vary systematically before and during major earthquakes (Smith, 1986) and in laboratory tests conducted under controlled conditions (Main *et al.,* 1990). This variation has been attributed to rock heterogeneity (Mogi, 1962) or heterogeneous stress distribution (Scholz, 1968). The most recent studies (Main *et al.,* 1990) have extended and unified these observations into a single negative correlation between b and the degree of stress concentration measured by the relative stress intensity factor K/K_c, where K_c is the fracture toughness.

A complete description of the fractal character of the seismotectonic data requires more than one fractal dimension or scaling exponent (Sornette *et al.* 1991; Cowie *et al.,* 1995), and these generally reflect different aspects of the scale invariance and need not be equal to or even positively correlated with one another. For example, the capacity dimension, D_o, estimated by the box-counting method (Feder, 1988), measures the space-filling properties of a fracture set with respect to changes in grid scale (Hirata, 1989a). The fractal relationship between the characteristic linear dimension of faults and the *b*-value (e.g., Turcotte, 1989) provides a measure of the relative proportion of large and small seismogenic faults (Aki, 1981; King, 1983) or cracks producing acoustic emission (Main *et al.,* 1990). The correlation dimension (D_C) (Grassberger and Procaccia, 1983) measures the spacing or clustering properties of a set of points and is often used to characterize the distribution of earthquake epicenters (Kagan and Knopoff, 1980; Hirata, 1989b) and hypocenter distributions of acoustic emissions in laboratory experiments (Hirata *et al.,* 1987).

This article reviews the previous results of our work (Oncel *et al.,* 1995, 1996a,b, 2001) that examine space-time variations in the correlation between the fractal characteristics of seismicity and faulting along the active fault zones of Japan and Turkey. Special note is made of unusual changes in the temporal correlation between seismicity distribution and *b*-value in the western segment of the NAFZ, from approximately 1975 to 1988, preceding the İzmit earthquake.

Regional Description

Japan

The Japanese islands are divided geologically into two different tectonic regimes at about 138° E longitude, roughly separating southwestern and northwestern Japan (Fig. 1a and b). This line falls roughly along the Itoigawa–Shizuoka tectonic line (ISTL), which is the tectonic boundary between southwestern and northeastern Japan and is also the western boundary of the Fossa–Magna region and the eastern boundary of the Japanese Alps. The ISTL is thought to represent an incipient subduction zone (Kobayashi, 1983; Nakamura, 1983) across which northeastern Japan (North American Plate) is subducting beneath southwestern Japan (Eurasian Plate).

In southwestern Japan, oblique subduction of the Philippine Sea Plate beneath the Eurasian Plate along the Nankai trough produces transpressional right-lateral offsets along the median tectonic line (MTL), in which the outer zone moves SW (Fig. 1a and b). The Philippine Sea Plate also descends beneath the North American Plate in the vicinity of central Japan and forms two TTT-type triple junctions. One is located near the southern end of the ISTL, where the Philippine, Eurasian, and North American plates meet, and the other is formed approximately 400 km to the east out in the Pacific ocean, where the Pacific, Philippine, and North American plates meet at the northern end of the Izu–Ogasawara arc.

Turkey

The tectonic environment of Turkey is also associated with complex multiplate interactions. The Anatolian Plate, for example, escapes westward along the North Anatolian

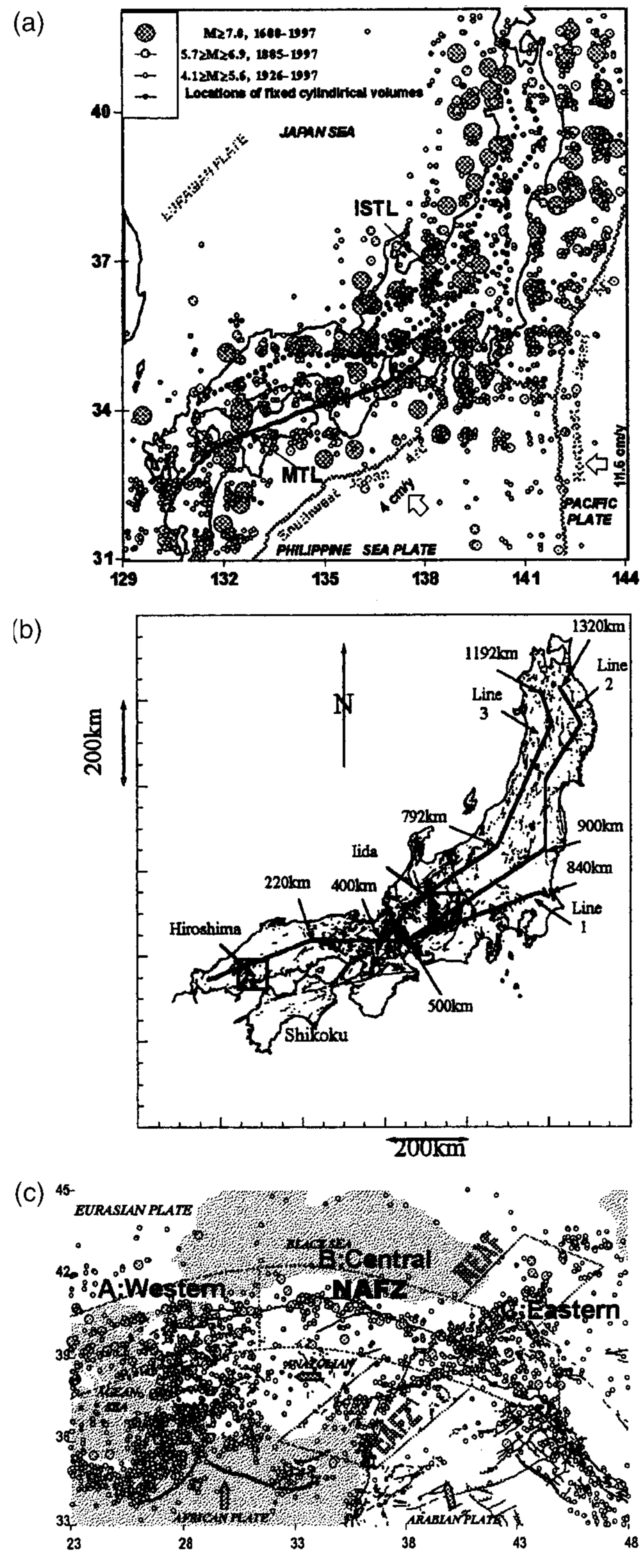

Figure 1. (a) Shallow mainshock seismicity data ($h < 20$ km) on land covering the period of time from 1600 to 1997. (b) Active fault map of Honshu and Shikoku. Locations of analysis lines 1 through 3 are shown. (c) The epicenter distribution of earthquakes that occurred between 1900 and 1992 in Turkey. The data are split into five seismotectonic zones labeled A–E.

Fault Zone (NAFZ) and the East Anatolian Fault Zone (EAFZ) because of the N–S compression exerted on the area by the collision of the African and Arabian plates to the south and the Eurasian plate to the north (Fig. 1c).

The deformation pattern in eastern Turkey consists of NE–SW left-lateral offsets along the EAFZ and NW–SE right-lateral conjugate strike-slip faults along the NAFZ resulting from N–S compression (Barka and Kadinsky-Cade, 1988; Taymaz *et al.,* 1991). The NAFZ, EAFZ, and the North East Anatolian Fault Zone (NEAFZ) are clearly defined by seismicity during the period of time extending from 1900 to 1992 (Fig. 1c).

Previous Studies

A recently completed study in Japan (Oncel *et al.,* 2001) examined the correlation between fractal properties of the active fault complex and the Gutenberg–Richter *b*-value. The study revealed that the correlation between D and b varies considerably throughout Japan and can be either positive or negative. Overall, D and b are negatively correlated. We interpreted that this would generally be the case because increased complexity in the active fault network (corresponding to increased fractal dimension) accommodates larger magnitude seismicity (lower b) along fault planes of relatively larger surface area. Significant positive correlations between b and D are also observed in Japan. Positive correlations occur in complex areas of the active fault network where the fractal dimension is highest. We interpreted that in these areas the probability of large-magnitude earthquakes decreases in response to increased fragmentation of the active fault network and there is increased possibility that stress release will take place along faults of smaller surface area.

Our studies also include an examination of the temporal evolution of seismicity in the western (between 24° and 31° E) and central (between 31° and 41° E) parts of the NAFZ (Oncel *et al.,* 1995, 1996a). Also, spatial variations of seismicity along the NAFZ, EAFZ, and NEAFZ were examined on the basis of their overall tectonic differences. A more objective examination in the spatial variations of seismicity along the NAFZ was conducted by dividing the fault zone into subregions, each of which contained 100 seismic events (Oncel *et al.,* 1996b).

The approach used in our research has been unique in that it explores the interrelationship between complex seismotectonic variables by comparing measures of their fractal properties. The results have potential applicability in the areas of earthquake hazard assessment. If, for example, interrelationships between the fractal characteristics of seismicity, active fault distributions, geodetic strain, topography, and other variables can be established, they may serve as a basis for seismotectonic classification and the identification of anomalous seismic behavior.

Methods of Analysis

Seismic *b*-Value

Estimates of the Gutenberg–Richter *b*-value are least biased when computed using the maximum likelihood method (Aki, 1965),

$$b = \log_{10} e/(\bar{m} - m_0 + 0.05), \tag{4}$$

where $\overline{m}$ is the mean magnitude of events of $M > m_0$, that is the threshold magnitude for which complete reporting is available. The seismic *b*-value is found to be negatively related to the mean magnitude and mean crack length (Main *et al.,* 1992). The value 0.05 is a correction constant that compensates for round-off errors. The 95% confidence limits for this estimate are $\pm 1.96b/\sqrt{n}$, where n is the number of earthquakes used to make the estimate. The *b*-value ranges between 0.5 and 1.6 in the present study. This yields typical confidence limits of ± 0.1–0.2 for a typical sample consisting of $n = 100$ earthquakes.

Capacity Dimension D_o

In the study we conducted in Japan (Oncel *et al.,* 2001) we used the box-counting method (e.g., Hirata, 1989a; Turcotte, 1989a) to evaluate the detailed size-scaling characteristics of active fault networks in Japan. The analysis was undertaken in 70- × 70-km areas of the fault network. Each area was covered by square boxes with sides of length r, and the number of boxes (N) containing part of the fault pattern was counted as r was decreased. Fractal behavior is implied when the number of occupied boxes (N) varies with the length of the box side (r) raised to some power ($-D$), as shown in equation (2).

$$N = Cr^{-D}. \tag{5}$$

In this relationship, D is the fractal dimension and is sometimes referred to as the capacity dimension, or box dimension. C is a constant. As defined by equation (5), D is a constant and therefore scale invariant.

Correlation Dimension, D_C

The correlation dimension, D_C, is determined using the correlation integral method. This method is often preferred, particularly when evaluating the scaling attributes of distributions of points such as epicenters. It provides a simple and reliable estimate of the fractal properties of point distributions (Kagan and Knopoff, 1980; Hirata, 1989b; Henderson and Main, 1992). The correlation dimension, D_C, is found using

$$D_c = \lim_{r \to 0} (\log C(r) / \log(r)), \tag{6}$$

where $C(r) = N/n$ is the correlation integral (Grassberger, 1983; Grassberger and Procaccia, 1983), N is the number of earthquake pairs in the particular analysis window separated by a distance less than r, and n is the total number of events analyzed. Here we also estimate the standard error, σ, found by linear regression of log C against log r. The percentage error obtained using this method is in general smaller than that of the b-value because it is based on a regression involving $n(n-1)/2$ individual two-point distances (r) rather than n in the case of earthquake magnitudes (m). The angular distance, r, in degrees between two events is calculated using the formula

$$r = \cos^{-1}(\cos\theta_1 \cos\theta_2 + \sin\theta_1 \sin\theta_2 \cos(\phi_1 - \phi_2)), \quad (7)$$

where (θ_1, ϕ_1) and (θ_2, ϕ_2) are the colatitudes (θ) and longitudes (ϕ) of the two events, respectively (Hirata, 1989). In the present study, the correlation dimension is defined by fitting a straight line to a plot of log $C(r)$ against log r (converted to a distance using $1° = 111$ km) as r tends to zero over a data range for the first 1.5 orders of magnitude for which the data were considered reliable. The lower bound may be determined by the epicentral resolution and the upper bound by the influence of the finite size of the study zone (Kagan and Knopoff, 1980). In the present study, the correlation plots in general exhibit scale invariance with parallel slopes in both the discrete and cumulative distributions between $0.7 < \log r < 2.2$ or $5 < r < 160$ km.

Space-Time Correlations: Results of Fractal Analysis

Japan

In our evaluation of the spatial distribution of variations between the capacity dimension of the active fault complex and b-value throughout Japan (Oncel *et al.,* 2001), we conducted detailed comparisons of D_0 and b along three regional lines that extend along the length of Japan (see Fig. 1b). Correlation coefficients between D_0 and b were computed at 20-km intervals along each line. A local measure of the correlation between b and D_0 was computed using a 160-km-long sliding window (Fig. 2). Overall, the correlation between b and D_0 is negative; however, an examination of the local correlation reveals areas of both positive and negative correlation.

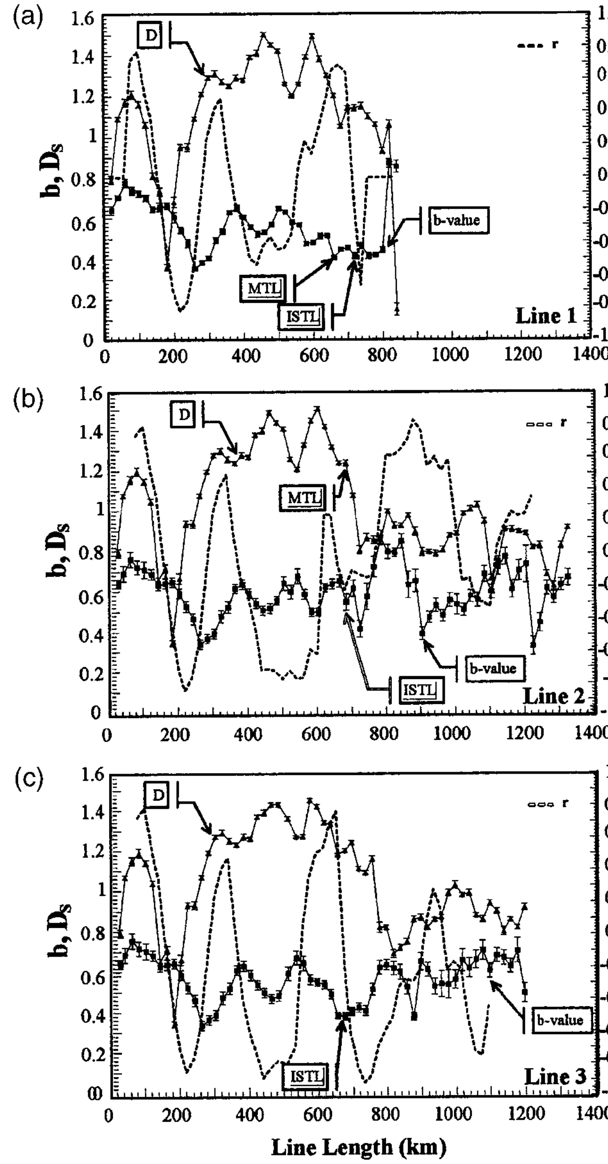

Figure 2. Variations in D_L and D_S are shown along lines 1–3. ATL: Akaishi tectonic line. ISTL: Itoigawa Shizuoka tectonic line. (a) Line 1 ends in central Japan. (b) Line 2 extends along the entire length of Honshu. (c) Line 3 extends along the entire length of Honshu.

Negative correlations are associated with a drop in b and parallel rise in D_0 (see Fig. 2). The drop in b suggests increased probability of seismicity of a larger magnitude. The parallel increase of D_0 is associated with denser and more complex regions of the active fault network. We suggest that this occurs because the greater density of faulting in the high D_0 areas accommodates rupture on interconnected faults of larger total surface area and therefore larger seismic magnitude.

Positive correlations arise from parallel variation of b and D_0. We interpret that the reduced probability of larger-magnitude earthquakes results from increased fault density, which allows stress to be released through lower-magnitude seismicity on smaller fault strands. Whether the correlation is positive or negative, there is an increase in D_0. However, b will rise or fall depending on the mode of failure within the dense fault system.

The differences in the time frames covered by seismicity and active fault data have a significant effect on the result. The active faults of Japan are considered to be active or potentially active if there has been some movement along the fault during the Quaternary. Whereas rupture may have had a tendency to occur on larger faults within the complex at one period of time, stress release along smaller fault strands may be prevalent at other times. A strong correlation is observed between Quaternary vertical displacements, surface elevation, and the fractal properties of topography (Wilson, unpublished data). However, topography and Quaternary vertical displacement do not correlate with short-term horizontal crustal strains measured over 10- and 100-yr time periods. Short-term horizontal crustal strain must have varied considerably over the 2.5-m.y. time frame of the Quaternary, so that at any particular instant in time, short-term strain patterns may differ considerably from net long-term strain.

We plan future work to evaluate the correlation of D_0 and recent crustal strain with the correlation dimension D_C throughout Honshu.

Turkey: Temporal Variations. The variation between b and D_C over time has been evaluated along the western and central subdivisions of the NAFZ. In both cases, a negative temporal correlation was obtained between b and D_C. Results obtained from the western part of the NAFZ from 1945 to 1988 (Fig. 3) are weakly negative ($r = -0.57$). Increases of b are generally paralleled by decreases of D_C. Oncel *et al.* (1995) suggested that the negative correlation in this instance might be an artifact of improved station coverage rather than a result of the underlying dynamics of strain release and remained cautious in their conclusion. Along the western segment of the NAFZ, which includes Istanbul and the Marmara Sea, b increases from approximately 0.7 to 1.4 over a 43-yr period of time extending from 1945 to 1988. The increases of b imply an increased event rate dominated by lower-magnitude seismicity. The data also reveal a significant change of behavior in the western part of the NAFZ between 1965 and 1975. If one considers only the data prior to 1965, the correlation is significantly negative (-0.92, see Fig. 4b). However, the variations of b and D_C after 1975 have a weak positive correlation (0.48, Fig. 4c). Oncel *et al.* (1996) undertook a similar comparison of b and D_C (Fig. 5) in the central part of the NAFZ (31°–41° E; Fig. 1c). Along

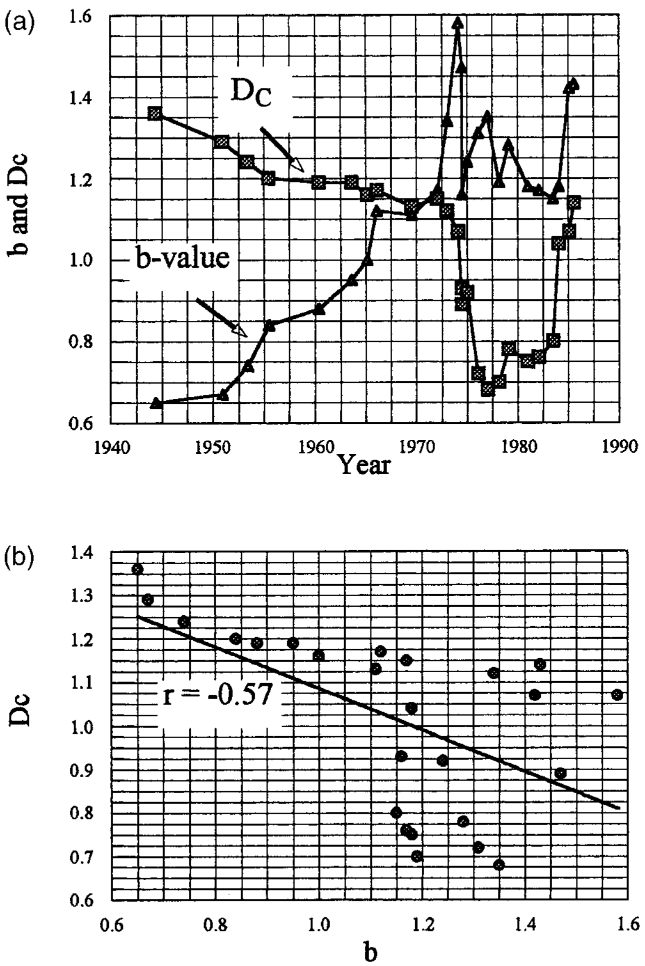

Figure 3. Comparison of b and D_C through the western part of the NAFZ. (a) Temporal variations of b-value and correlation dimension D_C. (b) Crossplot of b and D_C.

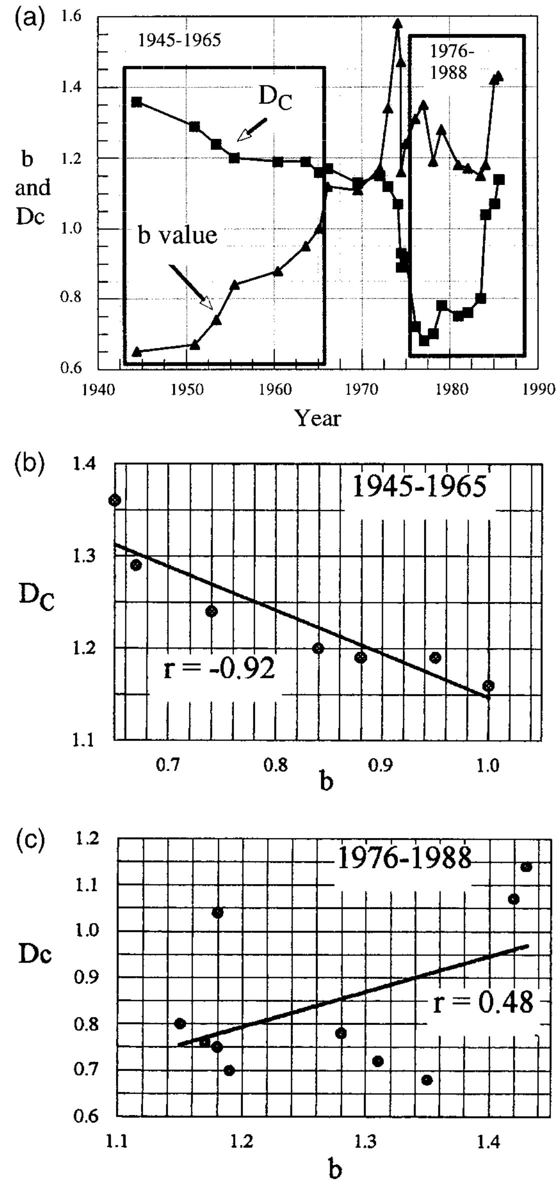

Figure 4. (a) Correlation between variations in b and D_C in the western NAFZ (a) are examined over the (b) 1945–1965 and (c) 1976–1988 time periods.

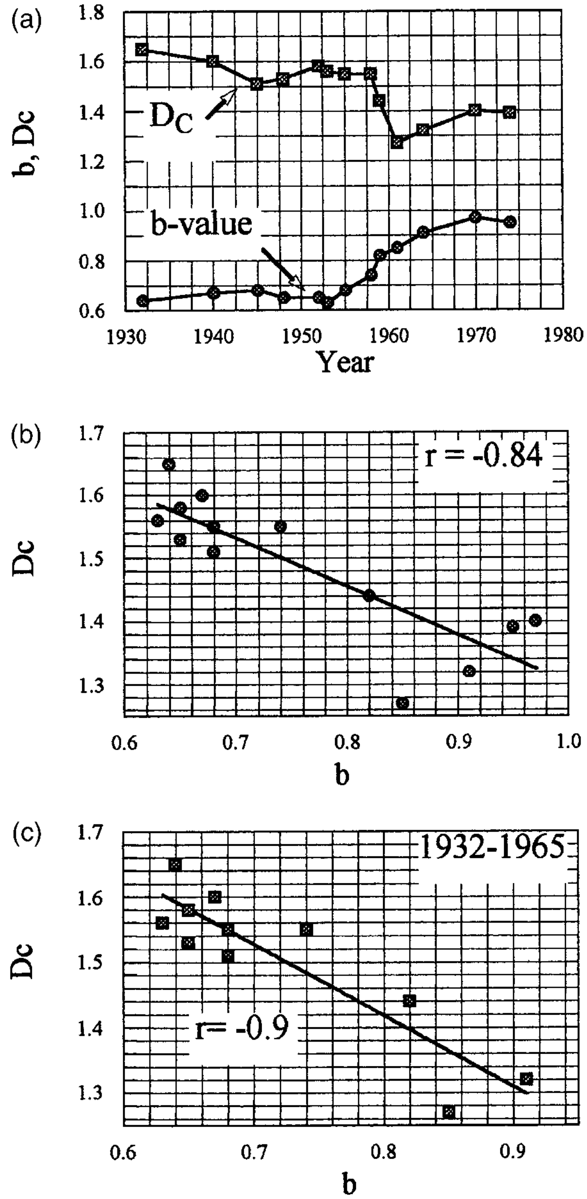

Figure 5. (a) Correlation between variations in b and D_C through the central NAFZ (a) are examined for the total period of observation extending from (b) 1931 to 1975 and for (c) 1931–1965.

this portion of the NAFZ, the period of analysis ended in 1975, and the event rate showed no dramatic increase because of increased station coverage (Fig. 5a). The negative correlation between b and D_C observed along the central part of the NAFZ was much stronger overall ($r = -0.84$, Fig. 5b) than that observed in the western part (-0.57, Fig. 3b). However, when the correlation is evaluated over the interval of time preceding 1965 (Fig. 5c), the correlation in the central part of the NAFZ ($r = -0.9$) is found to be similar to that observed in the western NAFZ (-0.92, Fig. 4b). The negative correlation between b and D_C is significant across the 1900-km span of the central and western NAFZ. Data from the western NAFZ after 1975 make a transition to positive correlation.

Seismic activity along the NAFZ has shown a general tendency to migrate westward during the time period 1900–1990 (Stein *et al.,* 1997). The decreased rate of occurrence of earthquakes of larger magnitude, inferred from an increase in b (0.65–0.95), observed in the central portion of the NAFZ up through the time period 1953–1975 might be associated with a shift in stress concentration into the western part of the NAFZ. The rise of b in the western NAFZ during the same time period is even greater (0.65–1.15); so there is no reason to suppose that stress transferred from the central to the western NAFZ was building up during that time period. The relationship of these changes with the 17 August 1999 İzmit earthquake ($M_s = 7.8$, 29.97° E and 40.76° N) and the 13 March 1992 Erzincan earthquake ($M_s = 6.8$, 39.61° E, 39.71° N) that occurred in the central NAFZ remains questionable until analysis of more recent data is completed. The sharp increase of the b-value along the western NAFZ that occurs between 1972 and 1974 (Fig. 3a) may be related to increased station density, because increased station density should yield increased numbers of low-magnitude events and an associated increase in b-value. However, this sudden increase in the b-value is followed by an equally sudden decrease from 1.6 to 1.15 between 1975 and 1977 (Fig. 3a). Thereafter, the b-value fluctuates about an average value of approximately 1.2 until 1985. D_C, on the other hand, drops suddenly from approximately 1.15 to 0.7 during the time period 1972–1977. This represents an increased tendency for seismicity to cluster and might also be produced by an increase in station coverage. Following 1977, D_C rises slightly (0.7–0.8) until about 1984. During the last 3 or 4 yr of the period of analysis, both b and D_C increase abruptly. During the time period 1976–1988, following the sudden changes of the mid-1970s, b and D_C exhibit weak positive correlation (Fig. 4c). The relationships between b and D_C preceding 1970 and following the mid-1970s are distinctly different. The increases of b occurring in the time period 1945–1965 level off during 1976–1988, and seismicity remains increasingly clustered (low D_C). From approximately 1985 to 1988, there are indications of a significant increase in both b and D_C, corresponding to increased levels of low-magnitude and more-scattered seismicity, respectively. This combination of factors—westward migration along with increased levels of low-magnitude seismicity and scattered (unclustered) epicenter distribution—might be indicators of increased seismic risk in the area. These variations reveal a level of complexity in seismic behavior that differs from previous reports that the b-value increases after a major earthquake up to a peak value and then decreases to a minimum at the time of occurrence of the next event (e.g., Gibovicz, 1973; Ma, 1978; Smith, 1986; Huang and Turbot, 1988; Main *et al.,* 1990). The ongoing analysis will track these changes into the present and provide a more definitive assessment of their interrelationship to the İzmit earthquake.

Turkey: Spatial Variations. Spatial variability between b and D_C is examined separately along the entire length of the

NAFZ. Oncel *et al.* (1996) undertook a detailed examination of the spatial variability of seismicity along the NAFZ for seven subdivisions (Fig. 6), each containing the same number of seismic events ($n = 100$). This analysis is restricted to the NAFZ, and regions one through seven extend from west to east along its length. Data used in this analysis include events of $M > 4.5$ recorded during the time interval 1900–1992. The variability between b and D_C along the length of the fault zone reveals divergence between b and D_C in the central NAFZ. D_C increases through the central part of the NAFZ, whereas the b-value decreases. The spatial variations yield a strong negative correlation ($r = -0.85$) between b and D_C (Fig. 7a).

The lowered b-value observed in the central NAFZ is associated with areas where there is a tendency for stress to build up over time and to be released by earthquakes that are less frequent but larger in magnitude. Conversely, higher the b-value observed to the west and east of the central NAFZ is considered indicative of low stress buildup accompanied by continued stress release in the form of numerous small-magnitude earthquakes. The high-D_C regions are associated with scattered, less-clustered epicenter distributions, whereas lower-D_C regions are associated with more-clustered epicenter distributions. The negative spatial correlation develops in response to an increase in stress concentration (lower b) and a decrease in epicenter clustering (increased D_C) through the convex-upward bend occurring in the central part of the NAFZ. Increased clustering (decreased D_C) and a tendency to experience smaller-magnitude seismicity (higher b) characterized both ends of the NAFZ during the period of time preceding 1975. It is apparently in these regions, where the NAFZ interacts with crosscutting fault systems, that stress is more easily dissipated in the form of larger numbers of smaller-magnitude earthquakes (i.e., higher b). The spatial variation of b and D_C reveals a change in the dynamics of plate interaction along the length of the NAFZ. However, the significance of those changes is not clearly understood. The areas of higher b and lower D_C (more clustered seismicity) may be the result of creeping parts of the fault zone, whereas higher D_C (less-clustered seismicity) and lower b may be related to asperities along the fault (Oncel and Wyss, 2000).

The spatial analysis provides a view of the long-term average characteristics of the b-value and D_C. The central NAFZ is an area where the probability of occurrence of larger-magnitude seismicity has been the greatest, on average, from 1900 to 1992. However, the preceding temporal analysis reveals that these properties are time variant. The changing relationship between b and D_C that occurs in the western NAFZ following 1975 represents an anomalous event. Recent conditions along the central NAFZ may suggest a cause. Recent deformation measured by Global Positioning System (GPS) (McClusky *et al.,* 2000) reveals maximum fault slip rates of 24 ± 2 mm/yr in the central part of the NAFZ, where D_C is higher (epicenter distribution is less clustered) and earthquake magnitudes are larger than average. This implies that, in general, there is greater fracture toughness in the central portions of the NAFZ. Oncel *et al.* (1996) examined the relation between b and D_C on a more regional scale that incorporated the Eastern Anatolian Fault Zone (EAFZ) (Figs. 1c and 7b). In the EAFZ, they found convergence between b and D_C similar to that found on the eastern and western ends of the NAFZ. Along the EAFZ and NAFZ, fault slip rates of 9 ± 2 mm/yr and 10 ± 2 mm/yr, respectively, were measured by GPS in the areas where b and D_C converge in value. The occurrence of rapid displacement along the central NAFZ was probably not released or compensated for by increased levels of scattered seismicity occurring in the western NAFZ. Had increased levels of low-magnitude seismicity been concentrated or clustered along the main fault strand, stress transferred into the western NAFZ might have been released more effectively, rendering the possibility of larger-magnitude earthquakes less likely.

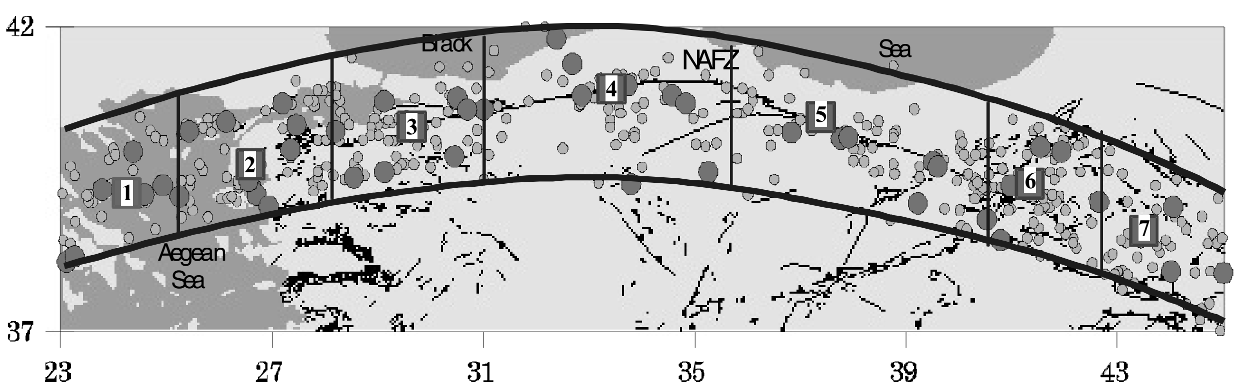

Figure 6. The NAFZ is been subdivided into seven regions, each of which contains 100 epicenters. Each area is bounded along strike by a meridian of longitude, and the north–south width is held constant. The central region along the NAFZ (region 4) is associated with a transition zone.

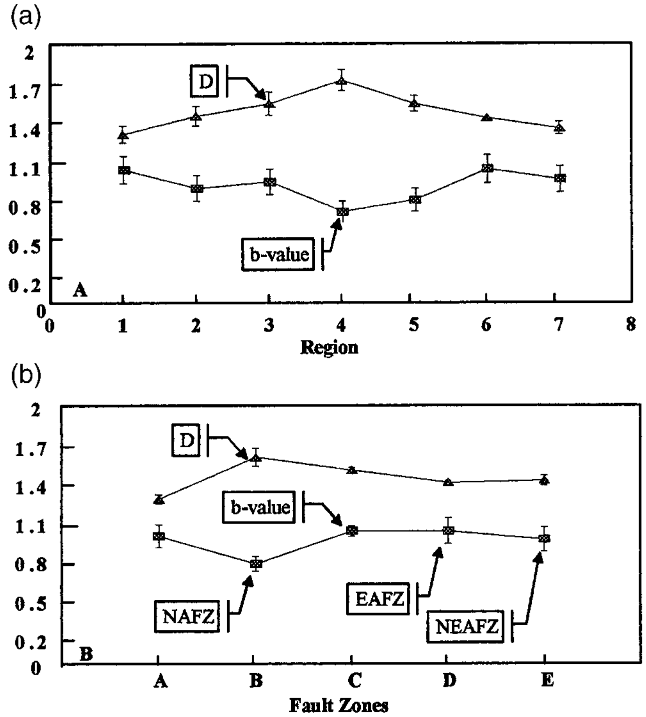

Figure 7. (a) Variations of b and D_C for zones 1–7 along the NAFZ. (b) 1 Variations of b and D_C observed along the AFZ for subdivisions A–E. A, western part of NAFZ; B, North Anatolian Fault; C, eastern part of NAFZ; D, East Anatolian Fault; E Northeast Anatolian Fault Zone.

Discussion

The relationship of the Gutenberg–Richter b-value to patterns of faulting and seismicity along convergent and transform plate boundaries provides information about the dynamics of plate interactions. In Japan, the spatial variations are interpreted to represent differences in the way in which stress is released within complex fault systems. In areas of positive correlation between b and D_0 (the capacity, or box dimension) the increased complexity and fragmentation of the fault system (increased D_0) may provide an abundance of small fault strands along which stress can be released through more frequent but lower-magnitude earthquakes (increased b). In areas of increased complexity in the active fault system (higher D_0) associated with larger-magnitude seismicity (lower b), stress release is interpreted to occur on fault planes of larger surface area.

In Turkey, the comparisons of b and D_C (correlation dimension of epicenter distribution) were followed through time and space along the length of the NAFZ. The variation between b and D_C over time was evaluated using sliding windows of 100 consecutive events of $M \geq 4.5$ in the time period 1900–1992. This leads to different time frames in the analysis of the western and central subdivisions of the NAFZ. The analysis in the western NAFZ is based on 375 events, which are distributed into 25 time windows beginning in 1944 and continuing until 1985. Analysis in the central NAFZ is based on only 175 events, which were divided into 14 time windows, that extend from 1932 to 1974. The duration of time represented by each point in the analysis varies from point to point to insure that values of b and D_C are derived from 100 events. Temporal variations of b and D_C, are negatively correlated during the time period 1940–1965. During that time there was a significant trend of increasing b-value followed by decreases in D_C. Unusual behavior is observed in the western NAFZ during the time period 1972–1977, which may be due to increased station density. However, the relationship between b and D_C from 1976 to 1988 (Fig. 4c) differs significantly from that associated with the time period 1945–1965. Seismicity suddenly became more clustered, whereas the b-value remained nearly constant during the time period 1976–1985. During the last 3 yr of the observation period (1985–1988), both b and D_C rose significantly. The changes that occurred between 1985 and 1988 might suggest that a sudden buildup of stress occurred in the region. The increase in b-value suggests that stress buildup underwent gradual release. Its behavior in the years immediately preceding the İzmit earthquake is currently under examination.

Spatial variation in the patterns of seismicity along the NAFZ reveals the presence of strong divergence in b and D_C through the central convex northward bend in the NAFZ. D_C increases and b decreases through this area. The negative correlation between b and D_C is associated with this divergence. The long-term (1900–1992) spatial averages suggest that the central NAFZ has increased risk of larger magnitude seismicity, whereas the western and eastern segments of the NAFZ are, on average, associated with reduced risk of higher-magnitude seismicity (higher b-value). However, recent slip rates reported through the central NAFZ are greater by a factor of two than those observed in the western NAFZ. This indicates that excess strain has recently been transmitted into the more slowly moving western NAFZ. Some of the differences between the central and western segments of the NAFZ may be related to differences in the mode of failure, as indicated by earthquake focal mechanisms and by the more densely spaced geodetic studies (Straub and Kahle, 1995, 1997; McClusky *et al.,* 2000). Along the eastern and central parts of the NAFZ, failure occurs under compression, whereas along its western extent, failure occurs through extension in the Aegean region (Fig. 1c).

The process of creep is usually associated with higher b-value, whereas asperities are often associated with lower b-value. The increases of b-value observed in the western NAFZ from 1975 to 1988 are associated with scattered (less-clustered) patterns of seismicity. Whereas this process may be associated with creep, its occurrence on the widely distributed pattern of seismicity may not have adequately accommodated stress release on the larger fault strands.

Conclusions

Temporal and spatial variations of the correlation dimension (D_C) and capacity dimension (D_0) show both negative and positive correlation to variations of the Gutenberg–Richter b-value. In the case of Japan, b may drop in intensely faulted areas (high D_0) because the more intensely faulted areas provide larger through-going faults along which stress release can occur. Thus, larger-magnitude earthquakes may be more likely to occur in these more intensely faulted areas. Positive variations between b and D_0 are also observed in Japan, and in this case it seems that more intensely faulted areas accommodate stress release on smaller fault strands.

Temporal analysis of variations between b and D_C in the western NAFZ make a transition from negative to slightly positive correlation between 1972 and 1976. A sudden drop of b-value precedes the change during a time when station density was increasing. Behavior from 1976 to 1988 is characterized by a tendency to have increased levels of low-magnitude seismicity on a widely scattered distribution of epicenters. The general trend of westward-migrating seismicity during the time period 1900–1990 (Stein *et al.,* 1997), with recent large slip rates occurring in the central NAFZ and lower slip rates in the western NAFZ, suggests that stress has been focused into the western NAFZ. The anomalous changes between b and D_C observed during the 1976–1988 time frame along the western segment of the NAFZ may have been a warning sign that increased levels of low-magnitude seismic events were not effectively releasing stress accumulation.

Acknowledgments

We would like to extend our appreciation to K. Kano, O. Nishizawa, and H. Kato for helpful discussions related to these studies. The authors also appreciate partial funding of their research through Japan AIST and STA Fellowships.

References

Aki, K. (1965). Maximum likelihood estimate of b in the formula $\log N = a - bm$ and its confidence limits, *Bull. Earthquake Res. Inst. Tokyo Univ.* **43,** 237–239.

Aki, K. (1967). Scaling law of seismic spectrum, *J. Geophys. Res.* **72,** 1217–1231.

Aki, K. (1981). A probabilistic synthesis of precursory phenomena, in *Earthquake Prediction, Maurice Ewing Series 4,* D. W. Simpson and P. G. Richards (Editors), American Geophysical Union, Washington, D.C., 566–574.

Aviles, C. A., C. H. Scholz, and J. Boatwright (1986). Fractal analysis applied to characteristics segment of the San Andreas Fault, *J. Geophys. Res.* **92,** 331–344.

Barka, A., and K. Kadinsky-Cade (1988). Strike-slip fault geometry in Turkey and its influence on earthquake activity, *Tectonics* **7,** 663–684.

Barton, C. C. (1994). Fractal analysis of the scaling and spatial clustering of fractures, in *Fractals and their Use in the Earth Sciences,* C. C. Barton and P. R. LaPointe (Editors), Plenum, New York (in press).

Barton, C. C., and P. A. Hseih (1989). Physical and hydrologic-flow properties of fractures, in *28th International Geological Congress Field Trip Guidebook T385*, American Geophysical Union, Washington, D.C., 36 pp.

Burrough, P. A. (1981). Fractal dimension of landscapes and other environmental data, *Nature* **294,** 241–242.

Cowie, P. A., D. Sornette, and C. Vanneste (1995). Multifractal scaling properties of a growing fault population, *Geophys. J. Int.* **122,** 457–469.

Feder, J. (1988). *Fractals*, Plenum, New York, 283 pp.

Gibowicz, S. J. (1973). Variation of the frequency-magnitude relation during the earthquake sequences in New Zealand, *Bull. Seism. Soc. Am.* **63,** 517–528.

Gilbert, L. (1989). Are topographic data sets fractal? *Pure Appl. Geophys.* **131,** 241–254.

Godano, C., and V. Caruso (1995). Multifractal analysis of earthquake catalogues, *Geophys. J. R. Astr. Soc.* **121,** 385–392.

Grassberger, P., and I. Procaccia (1983). Measuring the strangeness of strange attractors, *Physica* **9D,** 189–208.

Gutenberg, B., and C. F. Richter (1952). Earthquake magnitude, intensity, energy and acceleration, *Bull. Seism. Soc. Am.* **32,** 163–191.

Gutenberg, B., and C. F. Richter (1954). *Seismicity of the Earth and Associated Phenomena,* Princeton University Press, Princeton, New Jersey.

Hatton, C. G., I. G. Main, and P. G. Meredith (1993). A comparison of seismic and structural measurements of scaling exponents during tensile subcritical crack growth, *J. Struct. Geol.* **15,** 1485–1495.

Henderson, J., I. G. Main, P. G. Meredith, and P. R. Sammonds (1992). The evolution of seismicity-observation, experiment and a fracture-mechanical interpretation, *J. Struct. Geol.* **14,** 905–913.

Hirata, T. (1989a). Fractal dimension of fault systems in Japan: fractal structure in rock fracture geometry at various scales, *J. Pure Appl. Geophys.* **131,** 157–170.

Hirata, T. (1989b). Correlation between the b-value and the fractal dimension of earthquakes, *J. Geophys. Res.* **94,** 7507–7514.

Hirata, T., T. Satoh, and K. Ito (1987). Fractal structure of spatial distribution of microfracturing in rock, *Geophys. J. R. Astr. Soc.* **90,** 369–374.

Huang, J., and D. L. Turbot (1988). Fractal distributions of stress and strength and variations of b-value, *Earth Planet. Sci. Lett.* **91,** 223–230.

Jiang, J., and R. Plotnick (1998). Fractal analysis of the complexity of United States Coastlines, *J. Math. Geol.* **30,** 535–545.

Kagan, Y. Y., and L. Knopoff (1980). Spatial distribution of earthquakes: the two-point correlation function, *Geophys. J. R. Astr. Soc.* **62,** 303–320.

Kanamori, H., and D. L. Anderson (1975). Theoretical basis of some empirical relations in seismology, *Bull. Seism. Soc. Am.* **65,** 1073–1095.

King, G. (1983). The accommodation of large strains in the upper lithosphere of the earth and other solids by self-similar fault systems, *Pure Appl. Geophys.* **121,** 761–815.

Klinkenberg, B., and M. Goodchild (1992). The fractal properties of topography: a comparison of methods, *Earth Surface Processes and Landforms* **17,** 217–234.

Kobayashi, Y. (1983). On the initiation of the subduction of plates, *Earth Monthly* **5,** 510–514.

Korvin, G (1992). *Fractal Models in the Earth Sciences,* Elsevier, New York.

Ma, H. C. (1978). Variations of the b-values before several large earthquakes occurred in North China, *Acta Geophys. Sinica.* **21,** 433–462.

Main, I. G. (1992). Damage mechanics with long-range interactions: correlation between the seismic b-value and the fractal two-point correlation dimension, *Geophys. J. Int.* **111,** 531–541.

Main, I. G. (1996). Statistical physics, seismogenesis, and seismic hazard, *Rev. Geophys.* **34,** 433–462.

Main, I. G., P. G. Meredith, and P. R. Sammonds (1992). Temporal variations in seismic event rate and b-values from stress corrosion constitutive laws, *Tectonophysics* **211,** 233–246.

Main, I. G., P. G. Meredith, P. R. Sammonds, and C. Jones (1990). Influence of fractal flaw distributions on rock deformation in the brittle field, in *Deformation Mechanisms, Rheology and Tectonics,* R. J.

Knipe and E. H. Rutter (Editors), Geol. Soc. Lond. Spec. Publ. **54,** 81–96.

Mandelbrot, B. B. (1982). *The Fractal Geometry of Nature,* Freeman Press, San Francisco.

Mareschal, J. (1989). Fractal reconstruction of sea-floor topography, *Pure Appl. Geophys.* **131,** 197–210.

McClusky, S., S. Balassanian, A. Barka, C. Demir, S. Ergintav, I. Georgiev, O. Gurkan, M. Hamburger, K. Hurst, H. Kahle, K. Kastens, G. Kekelidze, R. King, V. Kotzev, O. Lenk, S. Mahmoud, A. Mishin, M. Nadariya, A. Ouzounis, D. Paradissis, Y. Peter, M. Prilepin, R. Reilinger, I. Sanli, H. Seeger, A. Tealeb, M. N. Toksöz, and G. Veis (2000). Global Positioning System constraints on plate kinematics and dynamics in the eastern Mediterranean and Caucasus, *J. Geophys. Res.* **105,** 5695–5719.

Mogi, K. (1962). Magnitude–frequency relation for elastic shocks accompanying fractures of various materials and some related problems in earthquakes, *Bull. Earthquake Res. Inst. Tokyo Univ.* **40,** 831–853.

Nakamura, K. (1983). Possible nascent trench along the Japan Sea as the convergent boundary between the Eurasian and North American plates, *Bull. Earthquake Res. Inst.* **58,** 711–722.

Okubo, P., and K. Aki (1987). Fractal geometry in the San Andreas fault system, *J. Geophys. Res.* **92,** 345–355.

Oncel, A. O., and Ö. Alptekin (1996). Complexity of the strike-slip faulting of Turkey (Abstracts), *Earthquake Res. Türkiye, Ankara-Turkey*, 21 pp.

Oncel, A. O., and M. Wyss (2000). The major asperities of the 1999 *M* 7.4 İzmit earthquake, defined by the microseismicity of the two decades before it, *Geophys. J. Int.* **143,** 501–506.

Oncel, A. O., Ö. Alptekin, and I. G. Main (1995). Temporal variations of the fractal properties of seismicity in the western part of the north Anatolian fault zone: possible artifacts due to improvements in station coverage, *Nonlinear Processes Geophys.* **2,** 147–157.

Oncel, A. O., I. G. Main, Ö. Alptekin, and P. A. Cowie (1996a). Spatial variations in the fractal properties of seismicity in the north Anatolian fault zones, *Tectonophysics* **257,** 189–202.

Oncel, A. O., I. G. Main, Ö. Alptekin, and P. A. Cowie (1996b). Temporal variations of the fractal properties of seismicity in the north Anatolian fault zone between 31°E and 41°E, *Pure Appl. Geophys.* **146,** 148–159.

Oncel, A. O., T. Wilson, and O. Nishizawa (2001). Size Scaling relations in the active fault networks of Japan and their correlation with Gutenberg–Richter *b*-Values, *J. Geophys. Res.* **106,** 21,827–21,841.

Robertson, M., and C. Sammis (1995). Fractal analysis of three-dimensional spatial distributions of earthquakes with a percolation interpretation, *J. Geophys. Res.* **100,** 609–620.

Rundle, J. B. (1989). Derivation of the complete Gutenberg–Richter magnitude-frequency relation using the principle of scale invariance, *J. Geophys. Res.* **94,** 12,337–12,342.

Sadovsky, M. A., T. V. Golubeva, V. F. Pisarenko, and M. G. Shnirman (1984). Characteristic dimensions of rock and hierarchical properties of seismicity, *Izv. Ac. Sci. USSR Phys. Solid Earth* **20,** 87–96 (English Translation).

Scholz, C. H. (1968). The frequency–magnitude relation of microfracturing in rock and its relation to earthquakes, *Bull. Seism. Soc. Am.* **58,** 399–415.

Scholz, C. H. (1994). *The Mechanics of Earthquakes and Faulting*, Cambridge U Press, Cambridge, 439 pp.

Smith, W. D. (1986). Evidence for precursory changes in the frequency–magnitude *b*-value, *Geophys. J. R. Astr. Soc.* **86,** 815–838.

Sornette, D., C. Vanneste, and A. Sornette (1991). Dispersion of *b*-values in Gutenberg–Richter law as a consequence of a proposed fractal nature of continental faulting, *Geophys. Res. Lett.* **18,** 897–900.

Stein, R. S., A. Barka, and J. Dieterich (1997). Progressive failure on the North Anatolian fault since 1939 by earthquake stress triggering, *Geophys. J. Int.* **128,** 594–604.

Straub, C., and H. Kahle (1995). Active crustal deformation in the Marmara Sea region, NW Anatolia, inferred from GPS measurements, *Geophys. Res. Lett.* **22,** 2533–2536.

Straub, C., and H. Kahle (1997). GPS and geologic estimates of the tectonic activity in the Marmara Sea region, NW Anatolia, *J. Geophys. Res.* **102,** 609–620.

Taymaz, T., J. Jackson, and D. McKenzie (1991). Active tectonics of the north and central Aegean, *Geophys. J. Int.* **106,** 433–490.

Turcotte, D. L. (1986). A fractal model of crustal deformation, *Tectonophysics* **132,** 361–369.

Turcotte, D. L. (1989a). Fractals in geology and geophysics, *Pure Appl. Geophys.* 171–196.

Turcotte, D. L. (1989b). *Fractals and Chaos in Geology and Geophysics,* Cambridge U Press, Cambridge, 221 pp.

Turcotte, D. L. (1992). *Fractals and Chaos in Geology and Geophysics,* Cambridge U Press, Cambridge.

Walsh, J. J., and J. Watterson (1993). Fractal analysis of fracture patterns using the standard box-counting technique: valid and invalid methodologies, Brevia, *J. Struct. Geol.* **15,** 1509–1512.

Weiss, J., and M. Gay (1998). Fracturing of ice under compression creep as revealed by multifractal analysis, *J. Geophys. Res.* **103,** 24,005–24,016.

Westeway, R. (1994). Present-day kinematics of the middle east and eastern Mediterranean, *J. Geophys. Res.* **99,** 12,071–12,090.

Wilson, T. H. (2001). Scale transitions in fracture and active fault networks, *Math. Geol.* **33,** no. 5, 591–613.

Wilson, T. H., and J. Dominic (1998). Fractal interrelationships between topography and structure, *Earth Surface Processes and Landforms* **23,** 509–525.

Wilson, T. H., K. Kano, and O. Nishizawa (in review). Interrelationships between topography, Quaternary vertical displacement, active faults and short-term horizontal crustal strain in Honshu, Japan, *Pure Appl. Geophys.* 49 pp.

Wu, S. (1993). Fractal strain distribution and its implications for cross-section balancing, *J. Struct. Geol.* **15,** 1497–1507.

Department of Geophysical Engineering—Turkey
Istanbul University
Istanbul, Turkey
(A.O.O.)

Department of Geology and Geography
West Virginia University
(T.H.W.)

Manuscript received 14 December 2000.